Available online at www.sciencedirect.com
ScienceDirect
Polymer 48 (2007) 174–182
polymer
www.elsevier.com/locate/polymer

Aliphatic poly(alkylene dithiocarbonate)s: Thermal properties and structural characteristics of poly(hexamethylene dithiocarbonate)

Corrado Berti [a], Annamaria Celli [a,*], Paola Marchese [a], Elisabetta Marianucci [a], Carla Marega [b], Valerio Causin [b], Antonio Marigo [b]

[a] *Dipartimento di Chimica Applicata e Scienza dei Materiali, Università di Bologna, Viale Risorgimento 2, 40136 Bologna, Italy*
[b] *Dipartimento di Scienze Chimiche, Università di Padova, Via Marzolo 1, 35131 Padova, Italy*

Received 11 July 2006; received in revised form 12 October 2006; accepted 16 November 2006
Available online 4 December 2006

Abstract

Aliphatic poly(alkylene dithiocarbonate)s are an interesting class of potentially biodegradable and biocompatible materials in analogy with their homologous poly(alkylene carbonate)s. In this paper, the properties of poly(hexamethylene dithiocarbonate) (SSR6) are compared to those of poly(hexamethylene carbonate) (HMC) in order to study the effect of the substitution of oxygen atoms with sulphur atoms in the polymer backbone. SSR6 presents a higher level of crystallinity and a faster crystallisation rate with respect to HMC. The melting temperature in SSR6 is about 60 °C higher, due to a solid–solid transition between phase I, stable at room temperature, and phase II, present at high temperature. HMC crystallises only in phase I and melts at a relatively low temperature (30 °C). The capacity of SSR6 to crystallise in phase II has been attributed to the higher flexibility and mobility of the chains containing –S–CO–S– groups with respect to the chains containing –O–CO–O– groups. The pure phase II in SSR6 has been obtained in isothermal conditions and its crystallisation rate and mechanism have been analysed.

Keywords: Aliphatic poly(alkylene dithiocarbonate)s; Solid–solid transition; Thermal characterisation

1. Introduction

Over the past 10 years, aliphatic poly(alkylene carbonate)s have attracted increasing interest as potentially biodegradable and biocompatible materials and numerous papers have been devoted to their possible applications. These polymers were found to be of interest for use in matrices for parental drug delivery systems, artificial skin, bone fixation plates, and ligature clamps [1–3]. In addition, some chemical modifications of the poly(alkylene carbonate)s have recently been reported. For example, the incorporation of pendent groups, like ester [1] or cyclic groups [4], or the functionalization with sulphate chain ends [5] allows the final properties to be regulated by the nature and amount of the modification. Moreover, the preparation of copolymers, based on trimethylene carbonate and glycolide [6], D,L-lactide [7,8], ε-caprolactone [7,9], ω-pentadecalactone [10,11], ethylene oxide [12], ethylene glycol [13], has been described. These copolymers are attractive for their mechanical properties and because they feature hydrolytic degradation and in vivo behaviour which can be modulated according to the chemical structure.

On the other hand, in order to modify the polycarbonate backbone and to obtain new properties, a different route can be followed: the substitution of oxygen atoms with sulphur atoms. Indeed, it is known that some engineering plastics containing sulphur atoms, such as poly(phenylenesulphide), poly(ethersulphone), and poly(sulphone), have excellent mechanical properties and resistance to heat and chemicals [14]. Moreover, the introduction of 4,4′-thiodiphenol improves the flexibility of polyarylate with poor impact strength [15] and the copolycondensation of 4,4′-thiodiphenol/bisphenol A with adipoyl dichloride improved the mechanical properties [16].

* Corresponding author. Tel.: +39 51 2093202; fax: +39 51 2093220.
E-mail address: annamaria.celli@mail.ing.unibo.it (A. Celli).

0032-3861/$ - see front matter © 2006 Elsevier Ltd. All rights reserved.
doi:10.1016/j.polymer.2006.11.035

Furthermore, polythioesters showed excellent properties, especially improved oxygen permeability compared with that of analogous polyesters [17].

The tendency to substitute the oxygen atoms with sulphur atoms is evident also in the recent efforts to prepare the sulphur analogues to the microbial polyesters well known as poly(hydroxyalkanoate)s [18–20]. The new polythioesters reveal some unexpected and interesting properties, as they are non-biodegradable polymers from renewable resources. This characteristic, which combines natural products with their persistence from microbial degradation, makes them promising biopolymers for new technical applications [21]. Moreover, a recent study also reports the synthesis of the sulphur analogous of some poly(alkylene dicarboxylate)s by lipase-catalysed thioesterfication [22]. Furthermore, it is noteworthy that the properties of biocompatibility of polythioesters which degrade hydrolytically into biological active compounds are useful for therapeutic purposes [23,24].

Given these recent trends, the synthesis of new poly(alkylene dithiocarbonate)s appears topical and significant for future developments. A series of poly(alkylene dithiocarbonate)s, represented by the general formula $[-(CH_2)_x-S-CO-S-]_n$, with x varying from 3 to 12, have been previously prepared by interfacial synthesis from aliphatic dithiols and phosgene [25].

Inside the family of the poly(alkylene dithiocarbonate)s, poly(hexamethylene dithiocarbonate) $[-(CH_2)_6-S-CO-S-]_n$ (SSR6) distinguishes itself by the other members of the series because of its complex thermal behaviour. Therefore, the study of the thermal and structural behaviour of SSR6, which requires peculiar attention and accuracy, is considered as an important start point for the wider study on the other aliphatic poly(alkylene dithiocarbonate)s. Moreover, comparison with the analogous poly(alkylene carbonate) $[-(CH_2)_6-O-CO-O-]_n$ (HMC) appeared interesting because now this latter is a commercial sample, thus characterised by practical applications.

Thus, in the present work we describe the thermal and structural characteristics of SSR6, in comparison with those of the analogous poly(alkylene carbonate); in a following paper the thermal and structural characterisations of all the samples of the series will be reported.

2. Experimental section

2.1. Materials

The synthesis of the poly(hexamethylene dithiocarbonate) (named SSR6, where 6 indicates the number of methylene groups in the monomeric unit) is described in Ref. [25]. M_W, determined by gel permeation chromatography (GPC) in $CHCl_3$ by using polystyrene standards for calibration, results equal to 8600 and the molecular weight distribution M_W/M_n equal to 2.3. The intrinsic viscosity, measured with Ubbelohde viscosimeter by using dilute solutions in chloroform at 30 °C, is 0.14 dl/g.

Poly(hexamethylene carbonate), $[-(CH_2)_6-O-CO-O-]_n$, is a commercial product by Aldrich, characterised by $M_n = 2000$. It is referred below as HMC.

2.2. Sample characterisation

The thermal analysis was carried out by means of a Perkin–Elmer DSC-7, calibrated with high-purity standards. The measurements were performed under nitrogen flow. In the non-isothermal analyses, both heating and cooling experiments were performed at different scanning rates (β) ranging from 1 to 20 °C/min. In order to cancel the previous thermal history, SSR6 and HMC were initially heated to 120 °C (first scan), kept at this temperature for 1 min and then cooled to −50 and 25 °C, respectively. During the cooling scan, measurements of the crystallisation temperature (T_{CC}) and the enthalpy of crystallisation (ΔH_{CC}) were made. After this thermal treatment, the samples were analysed by heating to 120 °C (second scan) and the cold crystallisation and melting temperatures (T_{Ch} and T_m) and the enthalpies of crystallisation and melting (ΔH_{Ch} and ΔH_m) were determined. Some other particular thermal treatments will be described in the text.

Isothermal crystallisation experiments were performed on SSR6 as follows: melting at 120 °C for 1 min, fast cooling to the selected crystallisation temperature T_C, isotherm at T_C for a time (t_{iso}) long enough to complete the crystallisation process, heating at 10 °C/min to 120 °C in order to observe the melting process. The T_C range varies from 75 to 82 °C.

Wide angle X-ray diffraction (WAXD) spectra were performed by a Philips X'Pert diffractometer. The heating and cooling programs were as follows:

For SSR6 in non-isothermal condition:

1. from room temperature (T_{room}) to the disappearance of crystallinity (T_m) at $\beta = 1$ °C/min. The spectra were recorded at 25 °C and then from 75 to 95 °C;
2. from T_m to T_{room} at $\beta = -5$ °C/min. The spectra were recorded at 75, 70, 65, 60 °C.

In isothermal condition:

3. fast cooling from 120 to 62 °C, isotherm for 30 min, and then the spectra were recorded at 64, 69, 75, 92, 100 °C;
4. fast cooling from 120 to 80 °C, isotherm for 30 min, and then the spectra were recorded at 85, 95, 105 °C.

The HMC sample was heated from 0 °C to T_m at $\beta = 10$ °C/min. The spectra were recorded at 10, 17, 24, 29, 32, 38, 60 °C, following the characteristic transitions of the heating scan of DSC experiment.

3. Results and discussion

3.1. Thermal behaviour in non-isothermal conditions

The DSC traces of SSR6, obtained after a complete melting, are reported in Fig. 1, curves (a) and (b). It is evident that during the cooling scan at the rate $\beta = -10$ °C/min (curve a), SSR6 crystallises originating a double exothermic peak, with the high exotherm at 71 °C and the low exotherm at 65 °C. The following heating scan ($\beta = 10$ °C/min) (curve b)

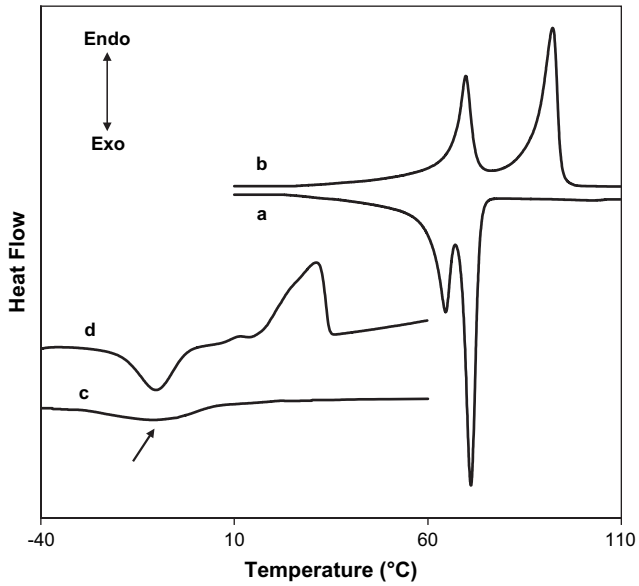

Fig. 1. DSC traces of SSR6 (curves a and b) and HMC (curves c and d). The samples have been melt, cooled at $\beta = -10$ °C/min (curves a and c) and then heated at $\beta = 10$ °C/min (curves b and d).

is characterised by the presence of two well distinct endothermic peaks, the low endotherm located at 69 °C and the high endotherm at 92 °C. The enthalpies of crystallisation and melting, calculated by integration of the sum of the two peaks, are about 60 J/g. Therefore, the polymer is a semicrystalline material, characterised by a complex crystallisation and melting behaviour.

The DSC curves of the homologous polycarbonate (HMC) are shown in Fig. 1, curves (c) and (d). In the cooling scan, HMC originates a broad and single crystallisation peak, characterised by low intensity, at $T_{CC} = -8$ °C (curve c, see the arrow). During the following heating scan, the crystallisation process takes place at about −10 °C, after which a wide melting process with a peak at $T_m = 31$ °C (curve d) is observed. It is evident that the crystallisation rate of HMC is notably slower than that of SSR6 and the transitions are shifted to lower temperatures. This behaviour could be due to the low molecular weight of the commercial HMC sample. However, DSC scans carried out on poly(hexamethylene carbonate) samples with higher molecular weight, reported by Kricheldorf and Mahler [26], show that also in this case the crystallisation and melting peaks take place at low temperatures ($T_{CC} = 16$ °C at $\beta = -10$ °C/min and $T_m = 62$ °C at $\beta = 20$ °C/min). A T_m value of 51 °C has been obtained by Pokharkar and Sivaram for a HMC sample with $M_n = 9550$ [27].

The higher melting temperature of the sample containing sulphur atoms with respect to the analogous oxygenated has been reported in the literature for aliphatic polydithiocarbonates [28] as well for other systems such as polythioethers and polythioesters with sulphur atoms in the main chain [29,30]. This behaviour is attributed to a higher packing efficiency in the crystalline lattice when the sulphur atoms are present [31]. This interpretation can also justify the faster crystallisation rate of SSR6 with respect to HMC.

As regards the melting process, it is worth remembering that the multiple behaviour of semicrystalline polymers has been studied intensely and can give rise to controversial interpretations [32]. The most common concepts invoked to explain the multiple behaviour are (i) a melting–recrystallisation–remelting process occurring during the calorimetric scan; (ii) existence of different crystal structures; (iii) presence of two populations of crystal lamellae or (iv) presence of crystals with different thermal stability. For numerous polymers, the first interpretation was found to be the most common: the low endotherm is due to the superimposition of the melting endotherm of the pre-existing crystals and the recrystallisation exotherm of the just molten material. The high endotherm, located at temperatures where the recrystallisation can no longer occur, is due to the melting of the crystals formed during the heating scan as dominant process.

A multiple melting behaviour arising from melting–recrystallisation–remelting during heating generally exhibits a strong dependence on the heating rate. At low heating rates, there is sufficient time for melting of initially formed crystals and recrystallisation during the heating scan: therefore, a shift of the high endotherm to high temperatures and an increment of its relative intensity occur. At high heating rates, the recrystallisation process cannot take place since the resident time of the molten crystals at temperatures where their recrystallisation could take place becomes too short.

In Fig. 2, the second heating scans of SSR6, crystallised during a cooling treatment at 20 °C/min from the melt, are displayed for heating rates ranging from 5 to 20 °C/min. It is noteworthy that the heating traces are independent of heating rate: the two endotherms retain their location, shape, and relative intensity. It is not possible to calculate the enthalpy of the two peaks separately, because they are not well separated; however, the total heat involved in the endothermic process remains constant ($\Delta H_m = 60$ J/g) in the three experiments. Therefore, these curves suggest that SSR6 does not present

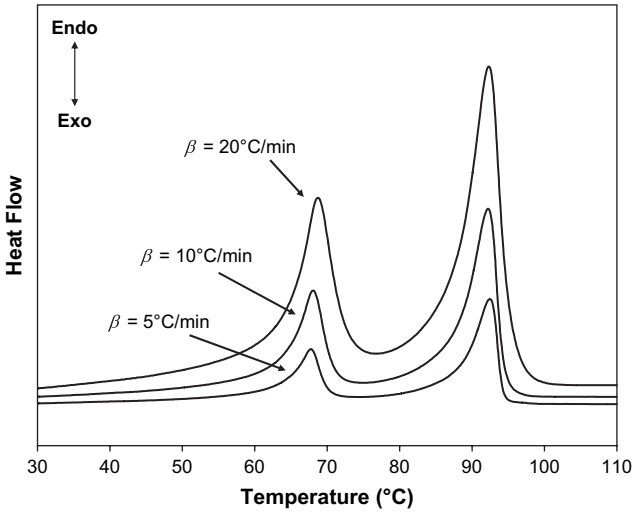

Fig. 2. DSC traces performed on SSR6, crystallised from the melt at 20 °C/min and heated at different heating rates, as indicated on the curves.

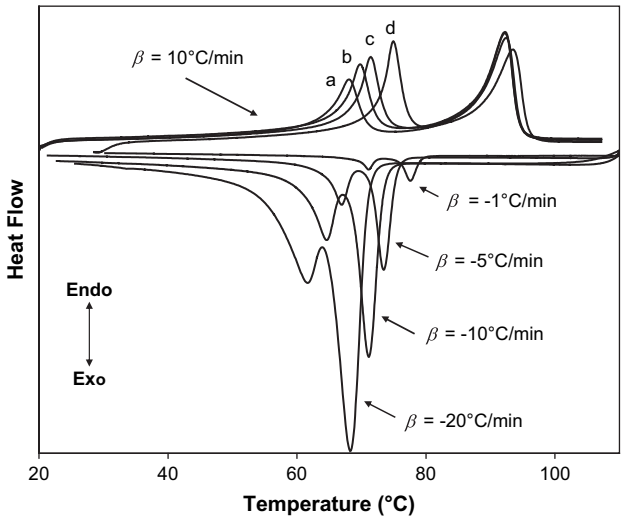

Fig. 3. DSC traces of SSR6, crystallised from the melt at the indicated cooling rates (β), and then heated at 10 °C/min. The heating curves have been performed after the cooling scan at (a) 20 °C/min; (b) 10 °C/min; (c) 5 °C/min; (d) 1 °C/min.

melting–recrystallisation–remelting processes during the heating scan in DSC.

Fig. 3 shows the cooling traces of SSR6 obtained at different rates ranging from $\beta = -1$ to -20 °C/min and the following heating traces recorded at the constant rate of 10 °C/min. Table 1 reports the temperatures of the low (L) and high (H) exothermal peaks of the cooling scans, called T_{CCL} and T_{CCH}, and the temperatures of the low and high endothermal peaks, named T_{mL} and T_{mH}. The ΔH values are calculated as the sum of the enthalpies of the two peaks.

In Fig. 3 it is possible to observe significant effects of the cooling rate on the thermal behaviour. In the cooling process, two peaks are always present and shift to lower temperatures with the increment of the cooling rate, in our opinion due to kinetic effects. However, their shape and relative intensity do not modify as a function of β, indicating that the extent of the two phenomena is independent of the scan rate. Indeed, ΔH_{CC} is constant (Table 1), whereas, in general, for a crystallisation process the decrement of the cooling rate should provide longer time for the growth of more perfect crystals and consequently an increment of ΔH_{CC}.

By observing the heating scans it is noteworthy that the low endotherm shifts to higher temperature as the cooling rate decreases, suggesting that slower the cooling process, greater the crystal perfection and, thus, higher the melting point. However, the high endotherm retains its position, independent of the cooling rate, and the total ΔH_m is constant (Table 1). This behaviour clearly suggests a difference in mechanism between low and high endotherms, and again indicates that the melting–recrystallisation–remelting process is not really probable. Therefore, the possible existence of two different crystal structures becomes one of the most significant hypotheses to justify the thermal behaviour of SSR6.

Table 1
DSC data calculated on the curves of Fig. 3 for SSR6

Cooling rate (°C/min)	T_{CCL} (°C)	T_{CCH} (°C)	ΔH_{CC} (J/g)	T_{mL} (°C)	T_{mH} (°C)	ΔH_m (J/g)
−1	71	78	64	75	93	60
−5	67	73	63	71	92	64
−10	65	71	62	70	92	60
−20	62	68	59	68	92	61

Fig. 4 shows the DSC traces obtained on SSR6 during a heating scan at 10 °C/min. Curve (b) is the result of a particular thermal treatment, 20 min of isotherm during the heating scan at the temperature corresponding to the end of the first endothermal peak (75 °C). After this, a certain increment of the temperature and enthalpy of the second melting peak may be noted. Generally, this behaviour is thought to be an indication of a recrystallisation process. For SSR6, instead, the interpretation of this result is fairly ambiguous, due to the previous observations. For this reason, the X-ray diffraction becomes a very powerful technique for understanding the thermal behaviour of the sample.

As far as the poly(hexamethylene carbonate) is concerned, in Fig. 5 the DSC curves obtained with the analogous treatments of Fig. 3 for SSR6 are reported. The corresponding DSC data are collected in Table 2. In the cooling scan, by changing β from -1 to -20 °C/min, the crystallisation peak shifts to lower temperatures and ΔH_{CC} value notably decreases, from 35 to 11 J/g. This behaviour is a clear indication that the crystallisation of HMC is prevented by high cooling rates [26]. Correspondingly, in the second heating scan the exothermal peak (T_{Ch}), due to the cold crystallisation, appears only after rapid cooling rates (curves a and b). The melting peak, located always at 31 °C, modifies its shape as a function of the cooling rate. In particular, a double melting peak is notable for very slow cooling rate (curve d). In the other curves (a–c), the melting process appears very broad. In any case, in the DSC traces there is no clear evidence of two distinct

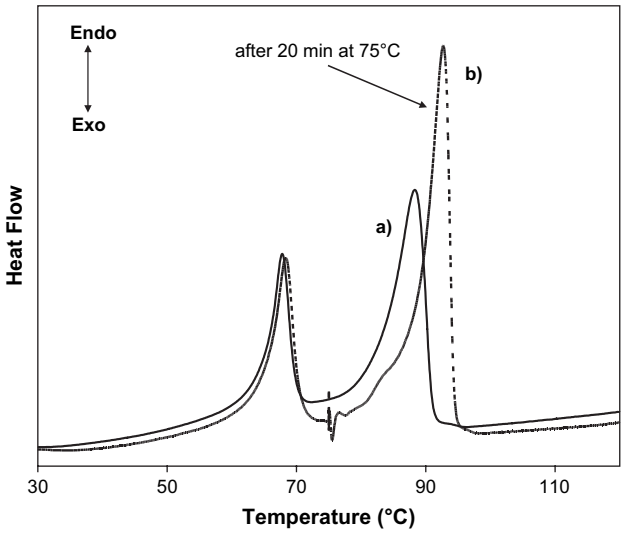

Fig. 4. DSC scans carried out on SSR6 crystallised from the melt at 20 °C/min. Curve (a): heating scan at 10 °C/min; curve (b): heating scan at 10 °C/min to 75 °C, isotherm at 75 °C for 20 min, and then heating scan to 120 °C.

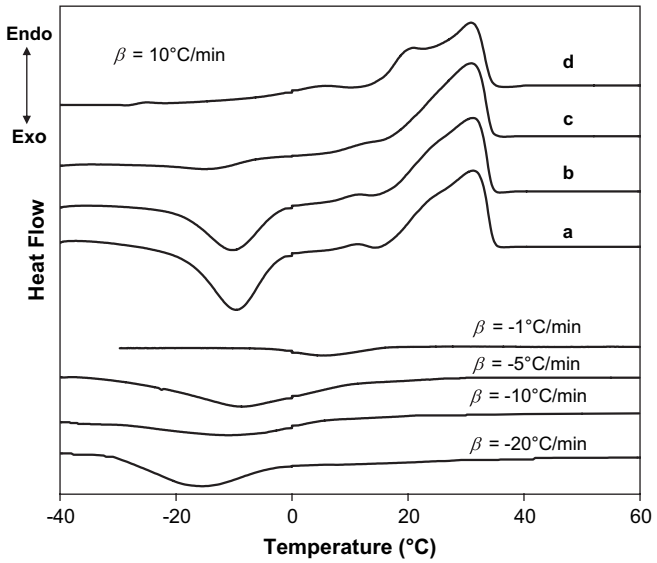

Fig. 5. DSC traces of HMC, crystallised from the melt at the indicated cooling rates (β), and then heated at 10 °C/min. The heating curves were performed after the cooling scan at (a) 20 °C/min; (b) 10 °C/min; (c) 5 °C/min; (d) 1 °C/min.

endothermal peaks, as in SSR6. These experimental results suggest that in HMC the melting process is probably due to melting–recrystallisation–melting phenomena.

In conclusion, from the results of the non-isothermal DSC analysis it is not possible to have conclusive findings about the thermal behaviour of the samples. Indeed, mainly for SSR6, the DSC analysis does not provide definitive chances to discriminate between melting–recrystallization–melting processes with respect to the melting or transformation of two different crystalline phases. Therefore, the X-ray diffraction analysis was considered as the right tool for a deeper investigation.

3.2. X-ray diffraction analysis

The wide angle X-ray diffraction analysis has been carried out on the virgin powders in order to verify the presence of more than one crystalline phase in the two samples, SSR6 and HMC, under investigation.

Fig. 6 reports the WAXD spectra, recorded during the heating scan on the SSR6 sample, which has not undergone any previous thermal treatment. At 25 °C, the spectrum is characterised by two main peaks at 19.1° and 24.3° of 2θ. The

Table 2
DSC data calculated on the curves of Fig. 5 for HMC

Cooling rate (°C/min)	T_{CC}[a] (°C)	ΔH_{CC}[a] (J/g)	T_{Ch}[b] (°C)	ΔH_{Ch}[b] (J/g)	T_m (°C)	ΔH_m (J/g)
−1	6	35	–	–	21–31	33
−5	−9	38	–	–	31	30
−10	−8	13	−10	18	31	32
−20	−17	11	−10	23	31	31

[a] Measured during the cooling scan.
[b] Measured during the heating scan.

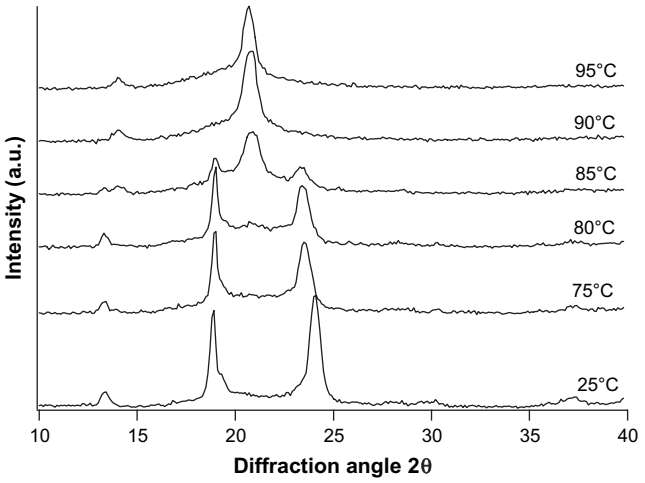

Fig. 6. SSR6 WAXD spectra recorded during the heating scan.

application of the least-squares fit procedure elaborated by Hindeleh and Johnson [33] gave a crystallinity of 57%.

During the heating scan, the two characteristic peaks gradually disappear and a new peak, located at 20.8° of 2θ, begins to appear starting from 80 °C. This is the only peak still present at $T \geq 90$ °C. Therefore, it is evident that two crystalline phases are present at different temperatures and a solid–solid transition takes place in a continuous way during the heating scan. Below, the crystalline phase present at room temperature will be referred to as phase I and the crystalline phase present at high temperature as phase II.

Fig. 7 shows the WAXD spectra recorded during the cooling scan from the melt: first of all it is worthwhile noting that the upturn of the base line at high 2θ values is probably due to the imperfect alignment of the surface of the sample after the melting. Actually, reflection WAXD spectra are susceptible to the lack of flatness on the surface of the material. The same explanation is to be invoked for the disappearing of the peak at 12–13° 2θ which was present in Fig. 6: indeed, a loss of resolution in reflection WAXD spectra is not unusual when the sample surface is not perfectly flat.

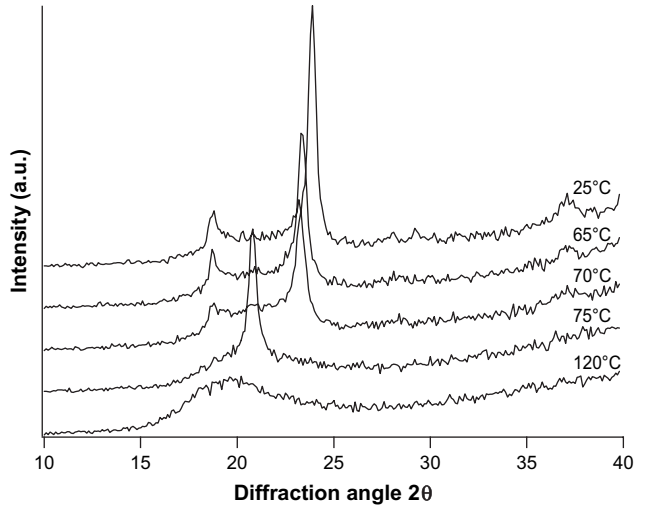

Fig. 7. SSR6 WAXD spectra recorded during the cooling scan from the melt.

Anyway, Fig. 7 shows that the SSR6 sample crystallises from the melt in phase II at 75 °C. Successively, at lower temperature (~70 °C), it undergoes the continuous transition from II to I phases. It is notable that at room temperature only phase I is present. Therefore, the solid–solid transition is completely reversible.

From Fig. 6 it is evident that the thermodynamic stability region for phase I is about from room temperature to 75 °C and for phase II from 90 °C to the complete disappearance of crystallinity.

By analysing these results together with those obtained by calorimetric analysis, it is possible to associate the endotherm at lower temperature in the DSC heating scan (Fig. 1, curve b) to the solid–solid transformation from phase I to II. Indeed, a solid–solid transition is a first-order transition, characterised by a calorimetric peak [34]. Moreover, the peak at higher temperature corresponds to the melting of phase II.

Correspondingly, during the cooling scan (Fig. 1, curve a) the higher peak is due to the crystallisation of phase II and the lower one is due to the II → I phase transition. The non-complete agreement between the transition temperatures observed in WAXD measurements with respect to those observed in the DSC analyses is due to the different temperature programs used. However, a good correspondence between the results is evident and the different nature of the two endothermic peaks observed in DSC traces is perfectly explainable.

In particular, previously we have observed that in Fig. 3 the low endotherm (peaks a–d) shifts to higher temperature with the decrement of the cooling rate. If the cooling rate is slow, the phase I crystals are probably more perfect and subsequently in the heating scan transform to phase II at higher temperature. Indeed, the dependence of the solid–solid transition temperature on the crystal size and lamellar thickness has already been observed for poly(tetrafluoroethylene) homopolymer [35] and copolymer [36]. The melting process of phase II, instead, seems to be independent of the temperature at which the crystals take origin from the transformation.

On the other hand, the high endotherm shifts to higher temperatures after the isothermal treatment described in Fig. 4, which is an isotherm of 20 min at a temperature correspondent to the end of the first endothermic peak. Therefore, only in this latter case does an improvement of the crystal perfection of phase II occur, causing an increment in the melting temperature. Probably, this process requires longer times than that available during the heating scan and, thus, the DSC heating rates used are probably too rapid to induce visible improvements in the crystalline phase II.

Fig. 8 shows the diffraction spectra recorded during the heating scan on the HMC sample. The X-ray diffraction pattern of the crystalline HMC measured at 24 °C (room temperature) is in agreement with the spectra reported in the literature [26,27]. Moreover, it is notable that HMC shows a crystalline structure similar to that of phase I in SSR6, though the degree of crystallinity is lower. Indeed, the application of the least-squares fit procedure elaborated by Hindeleh and Johnson [33] gave a 14% crystallinity value.

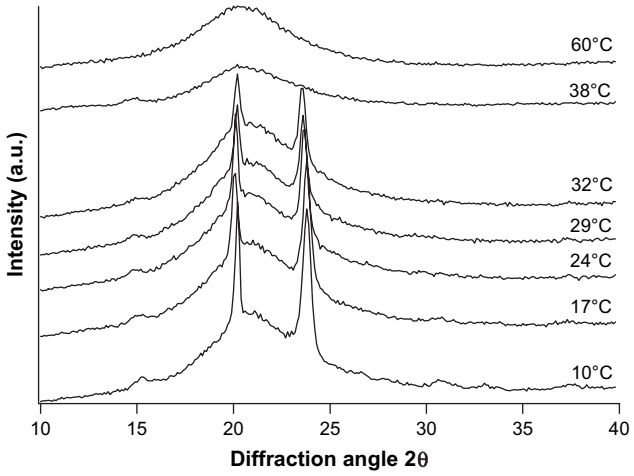

Fig. 8. HMC WAXD spectra recorded during the heating scan in non-isothermal measurements.

It is noteworthy that HMC retains its crystalline phase during the heating scan until melting. Therefore, the HMC sample does not undergo a solid–solid transition and its melting behaviour is clearly due to the rearrangements of the crystalline phase I.

To conclude, during the heating scan SSR6 gives rise to a solid–solid transformation, whereas HMC retains its crystalline structure until melting. The crystal–crystal transitions are relatively frequent among crystalline polymers: they have been observed, for example, in polyethylene [37,38], isotactic poly-1-butene [39], syndiotactic polypropylene [40], poly(tetrafluoroethylene) [35] and can be spontaneous or induced by specific treatments (for example, mechanical). They may be subjected to severe conformational and steric constraints, in particular when helical conformations are involved [41].

Therefore, in an initial approach, the different behaviour of SSR6 and HMC can be discussed in terms of chain mobility or impediments for chain packing. SSR6 distinguishes itself from HMC because of the presence of sulphur atoms instead of oxygen atoms. The sulphur atoms are larger than oxygen atoms and form –S–C– bonds longer than –O–C– bonds. As a consequence, the chain in SSR6 should be more flexible. Secondly, the sulphur atoms have lower electronegativity than the oxygen atoms: this induces a higher degree of polarisation of the carbonyl group in –S–CO– than in –O–CO–. Thus, the polar inter- and intramolecular interactions in SSR6 should be stronger than in HMC. As a result, in SSR6 the macromolecular chains are more free in their movements than in HMC and can rearrange by following the best energy pathways from one crystal lattice to the other. Moreover, the stability of the two crystalline forms is promoted by the interactions between the chains.

3.3. Thermal behaviour in isothermal conditions

Established the presence of a crystal–crystal transition in SSR6, the isothermal crystallisation process in SSR6 was analysed by DSC after a rapid cooling from the melt, by

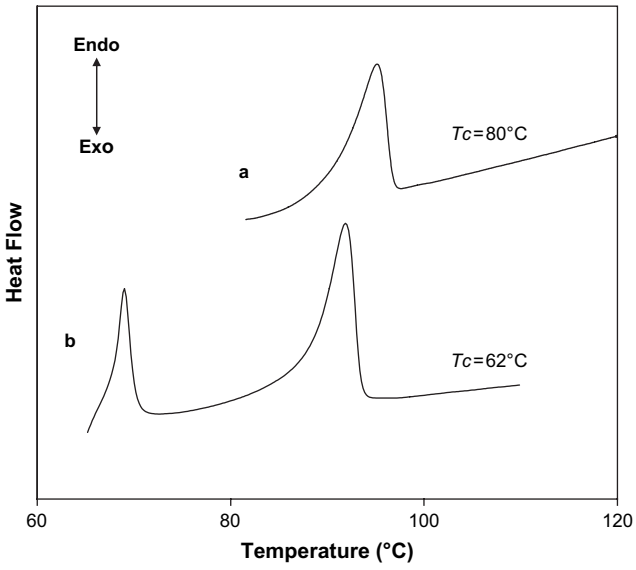

Fig. 9. Melting behaviour of SSR6 isothermally crystallised at the indicated T_C.

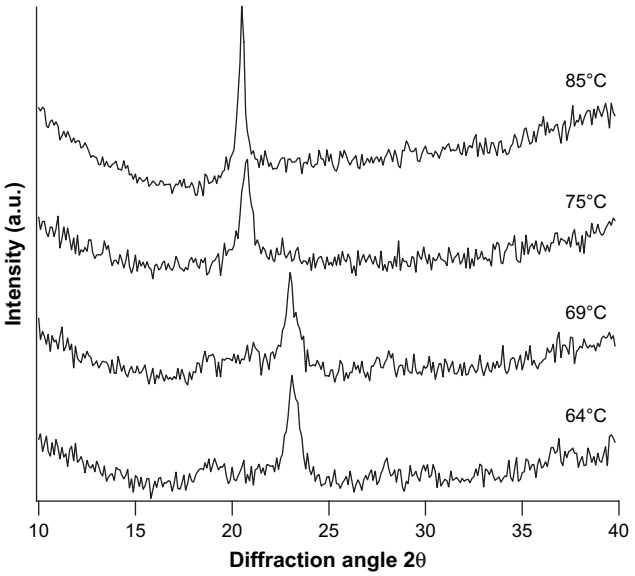

Fig. 11. SSR6 WAXD spectra recorded after isothermal crystallisation at $T_C = 62$ °C.

measuring the heat involved during crystallisation at T_C as a function of time. The choice of the T_C range investigated is crucial in order to obtain significant data. Indeed, the non-isothermal analysis has shown that the crystallisation from the melt is fairly rapid and always starts from phase II, while phase I grows only from phase II.

For example, Fig. 9 shows the endothermic peaks obtained by heating the samples at 10 °C/min after isothermal crystallisations at 80 and 62 °C, respectively.

Only one melting peak is present in curve (a) and two highly distinct processes are evident in curve (b). The WAXD profile, carried out on SSR6 after crystallisation from the melt at 80 °C shows that the polymer crystallises in phase II (Fig. 10). Moreover, the spectra recorded during the following heating scan shows that phase II remains up to the melting process. Consequently the single melting peak in curve (a) of Fig. 9 corresponds to the melting of the pure phase II.

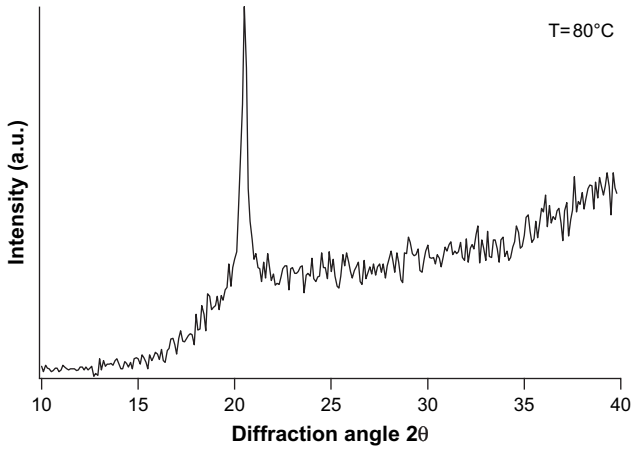

Fig. 10. SSR6 WAXD spectrum recorded after isothermal crystallisation at $T_C = 80$ °C.

On the other hand, Fig. 11 reports the WAXD spectra of the sample crystallised from the melt at $T_C = 62$ °C and, thus, heated until melting. At 64 and 69 °C, SSR6 shows profiles attributable to the form I, in spite of the low resolution of the diffraction peaks and the slight shift of the main signal to lower angles, probably due to thermal dilatation effect. At 75 °C, instead, the WAXD spectrum is that characteristic of phase II, which remains the only phase present until the melting process. Therefore, it is evident that the SSR6 sample at 62 °C is in phase I, formed from phase II during the cooling scan from the melt. During the following heating run, phase I transforms to phase II, originating the first endothermic peak at 69 °C in Fig. 9, curve (b). Moreover, the peak at 92 °C is the phase II melting process.

Thus, in order to study the isothermal crystallisation process from the melt, the T_C lower than about 70 °C must be avoided because in this case the exothermal signal measured in DSC could be attributed to the crystallisation process of phase II and to the II → I transformation, without the possibility of distinguishing these two phenomena. Only the formation of phase II, at $T_C \geq 75$ °C, can really be controlled. This is the reason why the T_C range selected is very narrow, varying from 75 to 82 °C.

The crystallisation of phase II was analysed quantitatively by following the macroscopic development of the polymer crystallinity by Eq. (1), obtained from the classical theory of Avrami for phase transformation kinetics [42]:

$$X_t = 1 - \exp[-K(t_C - t_0)^n] \quad (1)$$

X_t is the crystalline fraction and has been calculated from the ratio of the area of the exotherm peak in the thermogram at the time t_C and the total area of the crystallisation process. k is the overall kinetic constant, t_0 is the induction time, i.e. the time span before crystallisation begins at T_C. n is an exponent

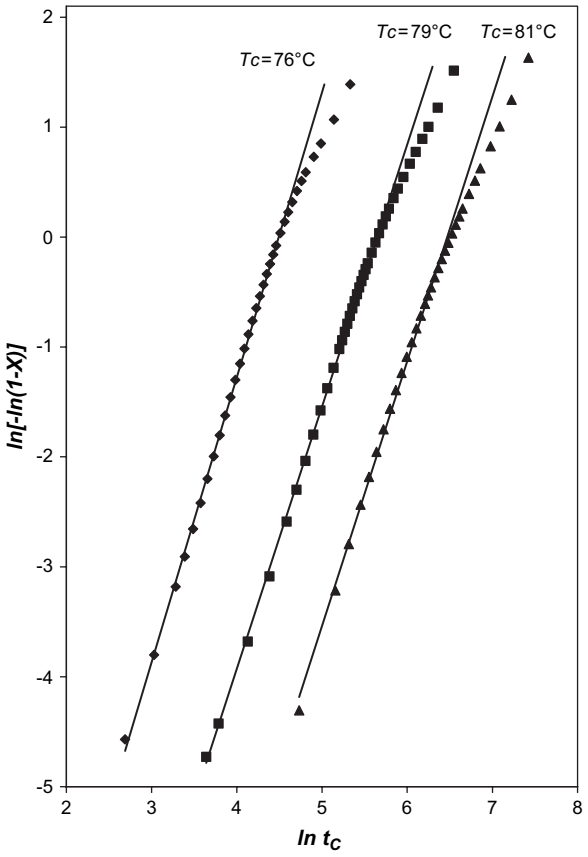

Fig. 12. Avrami plot for SSR6 crystallised at the indicated T_C.

whose value depends on the nucleation process and on the geometry of the crystals. K and n are determined, respectively, by the intercept and the slope of the straight line obtained in the plot of $\ln[-\ln(1-X_t)]$ versus $\ln(t_C - t_0)$ (Avrami plot). Fig. 12 shows some examples of the double logarithmic plot for SSR6 sample crystallised at three different T_C. Deviations from linearity are found at higher conversion degrees (>75%). They are frequently reported for crystallinities above 50% and attributed to secondary processes, such as increment of crystallinity, rejection of non-crystallisable portions of macromolecules and crystal perfection [43]. As regards the crystallisation mechanism, it is useful to analyse the Avrami exponent, whose values are around 2.6–3.0, typical of heterogeneous nucleation and three-dimensional growth.

To evaluate the crystallisation rate, the crystallisation half-time ($t_{1/2}$), defined as the time at which the polymer reaches a crystalline fraction equal to 0.5, has been used. This value was obtained by subtracting the induction time (t_0) from t_C. In particular, the reciprocal of $t_{1/2}$ is proportional to the crystallisation rate. Fig. 13, which describes the trend of $(1/t_{1/2})$ as a function of T_C, shows that the rate of crystallisation decreases with the increment of T_C. As the conventional bell-shaped curve is expected, only the portions of the crystallisation rate curves at high T_C, near the melting point, are detectable by DSC. This result will be used in a subsequent paper to compare the crystallisation rates of SSR6 with those of analogous

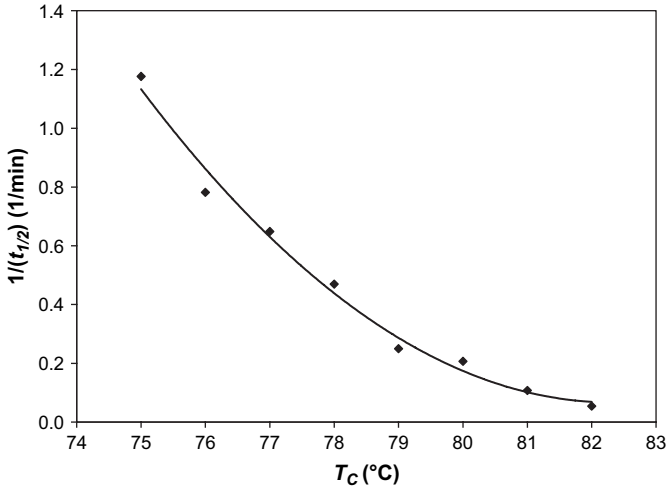

Fig. 13. Crystallisation rate vs. T_C for phase II of SSR6.

polydithiocarbonates with different number of methylene units.

Table 3 reports some data of the pure phase II. The crystallisation and melting enthalpies, which cannot be calculated by non-isothermal DSC analysis because of the superimposition of peaks, present values variable from about 35 to 20 J/g. In particular, the values decrease with the increment of T_C as the crystallisation process slows down. Also T_m presents an increment of about 4–5 °C, due to the improvement of the crystal perfection. An initial evaluation of the equilibrium melting temperature of phase II by using the Hoffman–Weeks extrapolation [44] provides a T_m value of 120 °C.

Analogous results on the pure phase I of SSR6 are difficult to obtain. Indeed, phase I grows only from the crystals of phase II and not by nucleation from the melt. Therefore, the mechanism of phase I formation appears more complex. Moreover, the determination of the transformation rate is experimentally complicated by the narrow temperature range which separates the crystal transformation from the crystallisation and melting of phase II.

Isothermal treatments on HMC were not carried out due to its slow crystallisation kinetics.

Table 3
Isothermal crystallisation data of phase II

T_C (°C)	t_{iso}[a] (min)	$t_{1/2}$ (min)	ΔH_C (J/g)	T_m (°C)	ΔH_m (J/g)
75	3.20	0.85	33	93.0	30
76	5.00	1.28	37	92.6	30
77	6.00	1.54	31	93.5	29
78	10.0	2.13	27	93.6	28
79	14.0	4.00	25	94.4	26
80	20.0	4.83	25	95.1	25
81	36.0	9.29	20	96.3	23
82	60.0	18.4	20	97.4	22

[a] Experimental time of isotherm at T_C, necessary to reach the complete crystallisation.

4. Conclusions

The thermal and structural properties of poly(hexamethylene dithiocarbonate) (SSR6) and poly(hexamethylene carbonate) (HMC) have been analysed and compared in order to study the effect of the substitution of oxygen atoms with sulphur atoms in the polymer backbone. It is noteworthy that the two samples present a notably different behaviour.

SSR6 is a material with higher degree of crystallinity (about 60% vs. 15%) and a faster crystallisation rate with respect to HMC. These characteristics are attributed to the higher packing efficiency in the crystalline lattice when sulphur atoms are present.

Moreover, the DSC thermograms of SSR6 are characterised by multiple transitions, whose nature has been clearly understood from WAXD analysis, with a solid–solid transition taking place. Phase I, stable at room temperature, transforms into phase II at about 60–70 °C, depending on the thermal cycle. Only phase II is present at high temperature and then melts at about 90 °C. The transition is completely reversible. During the cooling from the melt, SSR6 crystallises in form II, which then transforms into form I.

HMC, instead, does not show any crystal–crystal transformation, but only a crystalline phase corresponding to form I of SSR6. The fact that only SSR6 is able to rearrange into phase II has been explained by considering the higher flexibility and mobility of the chains containing −S−CO−S− groups with respect to the chains containing −O−CO−O− groups. Due to the presence of this crystal transformation, SSR6 has a melting temperature of about 60 °C higher than HMC (90 °C vs. 30 °C).

Isothermal crystallisation studies, performed in a narrow T_C range, allow only the pure phase II to be obtained. The crystallisation rate and mechanism have been determined; the extrapolation of the melting temperatures gives a value of equilibrium melting temperature of 120 °C.

As a conclusion, the significant differences in the thermal behaviour between the two samples highlight the good physical properties of SSR6, which could become an attractive material for new applications.

References

[1] Liu Z-L, Zhou Y, Zhou R-X. J Polym Sci Part A Polym Chem 2003;41:4001–6.
[2] Zhu KJ, Hendren RW, Jensen K, Pitt CG. Macromolecules 1991;24:1736–40.
[3] Schindler A, Jeffcaat R, Kimmel GL, Pitt CG, Wall ME, Zweidinger R. In: Pearce EM, Schaefgen JR, editors. Contemporary topics in polymer sciences, vol. 2. New York: Plenum; 1997.
[4] Chen X, McCarthy SP, Gross RA. Macromolecules 1997;30:3470–6.
[5] Atthoff B, Nederberg F, Hilborn J, Bowden T. Polym Prep (Am Chem Soc Div Polym Chem) 2005;46:473–4.
[6] Zurita R, Puiggali J, Franco L, Rodriguez-Galan A. J Polym Sci Part A Polym Chem 2005;44:993–1013.
[7] Pego AP, Van Luyn MJA, Brouwer LA, van Wachern PB, Poot AA, Grijpma DW, et al. J Biomed Mater Res Part A 2003;67:1044–54.
[8] Buchholz B. J Mater Sci Mater Med 1993;4:381–8.
[9] Albertsson A-C, Eklund M. J Appl Polym Sci 1995;57:87–103.
[10] Kumar A, Garg K, Gross RA. Macromolecules 2001;34:3527–33.
[11] Focarete ML, Gazzano M, Scandola M, Kumar A, Gross RA. Macromolecules 2002;35:8066–71.
[12] Feng Y, Zhang S. J Polym Sci Part A Polym Chem 2005;43:4819–27.
[13] Zhang Y, Zhuo R-x. Biomaterials 2005;26:2089–94.
[14] Harris JE, Johnson RN. Polysulfones. Encyclopedia of polymer science and engineering, vol. 13. New York: John Wiley & Sons; 1985.
[15] Chen T, Wang D, Chiu W, Chen L. Angew Makromol Chem 1996;239:133–40.
[16] Hirano H, Tanaka M. Angew Makromol Chem 1999;267:57–62.
[17] Hirano H, Watase S, Tanaka M. J Appl Polym Sci 2005;96:508–15.
[18] Thakor N, Letke-Eversloh T, Steinbuechel A. Appl Environ Microbiol 2005;71:835–41.
[19] Lutke-Eversloh T, Steinbuechel A. Biopolymers 2003;9:63–80.
[20] Doi Y. Nat Mater 2002;1:207–8.
[21] Steinbuchel A. Curr Opin Biotechnol 2005;16:607–13.
[22] Weber N, Bergander K, Fehling E, Klein E, Vosmann K, Mukherjee KD. Appl Microbiol Biotechnol 2006;70:290–7.
[23] Uhrich KE. PCT Int Appl, WO 2003-US3718, 2003.
[24] Ulrich KE. PCT Int Appl, WO 2003-US3818, 2003.
[25] Pilati F, Marianucci E, Berti C, Manaresi P, Della Fortuna G. Polym Commun 1990;31:431–4.
[26] Kricheldorf HR, Mahler A. Polymer 1996;37:4383–8.
[27] Pokharkar V, Sivaram S. Polymer 1995;36:4851–4.
[28] Montaudo G, Pugliesi C, Berti C, Marianucci E, Pilati F. J Polym Sci Polym Chem Ed 1989;27:2277–90.
[29] van Krevelen DW. Properties of polymers. 3rd ed. Amsterdam: Elsevier; 1990.
[30] Marvel CS, Kotch A. J Am Chem Soc 1951;73:1100–2.
[31] Riande E, Guzman J, Roman JS. J Chem Phys 1980;72:5263–8.
[32] Wunderlich B. Crystal melting. Macromolecular physics, vol. 3. New York: Academic; 1980.
[33] Hindeleh AM, Johnson DJ. J Phys D Appl Phys 1971;4:259–63.
[34] Cheng SZD, Keller A. Annu Rev Mater Sci 1988;28:533–62.
[35] Marega C, Marigo A, Causin V, Kapeliouchko V, Di Nicolò E, Sanguineti A. Macromolecules 2004;37:5630–7.
[36] Weeks JJ, Sanchez IC, Eby RK, Poser CI. Polymer 1980;21:325–31.
[37] Rastogi S, Kurelec L. J Mater Sci 2000;35:5121–38.
[38] Wittmann JC, Lotz B. Polymer 1989;30:27–34.
[39] Marigo A, Marega C, Cecchin G, Collina G, Ferrara G. Eur Polym J 2000;36:131–6.
[40] De Rosa C, Auriemma F, Vinti V. Macromolecules 1998;31:7430–5.
[41] Lotz B, Mathieu C, Thierry A, Lovinger AJ, De Rosa C, Ruiz de Ballesteros O, et al. Macromolecules 1998;31:9253–7.
[42] Avrami M. J Chem Phys 1939;7:1103–12. 1940;8:212–24; 1941;9:177–84.
[43] Wunderlich B. Crystal nucleation, growth, annealing. Macromolecular physics, vol. 2. New York: Academic; 1980.
[44] Hoffman JD, Weeks J. J Res Natl Bur Stand (A) 1962;66:13–28.